Bull. Mater. Sci., Vol. 37, No. 4, June 2014, pp. 809–813. © Indian Academy of Sciences.

Magnetization reversal and ferrimagnetism in $Pr_{1-x}Nd_xMnO_3$

SANJAY BISWAS, MOMIN HOSSAIN KHAN and SUDIPTA PAL*
Department of Physics, University of Kalyani, Nadia 741 235, India

MS received 23 May 2013; revised 12 July 2013

Abstract. Detailed magnetic properties of $Pr_{1-x}Nd_xMnO_3$ (x = 0·3, 0·5 and 0·7) have been reported. All the samples crystallize in orthorhombic perovskite structure with *Pnma* space group. Magnetization measurements under field cooled (FC) protocal reveal magnetization reversal at low temperatures and low magnetic field. This indicates clear evidence of two magnetic sublattices aligned opposite to each other. There is a well-defined maximum around 48 K in the x = 0·7 sample (i.e. $Pr_{0.3}Nd_{0.7}MnO_3$) in the χ' value which is identified as paramagnetic to ferrimagnetic transition. The peak value shifts to higher temperature with decrease of x and width of the maximum broadened. It is also observable that with decrease of Nd, both the value of χ' and χ'' decrease. An attempt is made to explain the magnetization reversal within the framework of available models.

Keywords. Manganites; magnetic transition; exchange interaction; magnetization reversal.

1. Introduction

The subject of magnetization reversal in rare earth oxides has received considerable attention in recent years. The magnetic moments of rare earth ions are polarized due to the coupling with the Mn subsystem resulting in a noticeable anisotropic contribution to the low-temperature magnetic and thermodynamic properties of the manganites as observed in $PrMnO_3$ and $NdMnO_3$ (Hemberger *et al* 2004; Hong *et al* 2012). In rare earth manganites, if rare earth ion is replaced by another rare earth ion, interesting changes in transport and magnetic properties occur. In $Nd_{1-x}Ce_xMnO_3$, Nd is substituted by Ce and these types of manganites contain Mn^{3+} and Mn^{2+} sublattices. DE interaction between these sublattices explains the FM, AFM nature with temperature and low-temperature magnetization reversal phenomena (Zhang *et al* 2005). This kind of magnetic phenomena have also been observed in $GdCrO_3$ (Yoshii 2001), $Gd_{0.7}Ca_{0.3}Mn_{1-x}Cr_xO_3$ (Biswas *et al* 2013), $Bi_{0.3}Ca_{0.7}Mn_{0.75}Cr_{0.25}O_3$ (Zhang *et al* 2012), Sr_2YbRuO_6 (Singh and Tomy 2008), $La_{1-x}Gd_xMnO_3$ (Hemberger *et al* 2004), $La_{0.5}Gd_{0.5}CrO_3$ (Sharma *et al* 2010), $La_{1-x}Pr_xCrO_3$ (Yoshii *et al* 2001) and $La_{1-x}Ce_xCrO_3$ (Manna *et al* 2010). In $GdCrO_3$, rare earth Gd and transition metal Cr are canted or aligned in opposite direction. Again in $Gd_{0.7}Ca_{0.3}Mn_{1-x}Cr_xO_3$, Gd is aligned against Cr and Mn ions. In $Bi_{0.3}Ca_{0.7}Mn_{0.75}Cr_{0.25}O_3$, Mn and Cr are canted in opposite direction and Ru and Yb are canted in opposite direction in Sr_2YbRuO_6. Again for being La^{3+} non-magnetic, reversal of magnetization in $La_{0.5}Gd_{0.5}CrO_3$ is due to canted opposite direction magnetic moment of Gd and Cr. For all these compounds, reversal of magnetization phenomena are explained considering two sublattice systems which are aligned antiparallel to each other. The magnetization reversal phenomena in $YFe_{1-x}Mn_xO_3$ (Mandal *et al* 2013) can be explained by random occupation of magnetic ions and different magnetic interactions like Fe–O–Fe, Fe–O–Mn and Mn–O–Mn. Again in $NdMnO_3$ (Hong *et al* 2012), the negative magnetization phenomena has been explained by considering Nd^{3+} and Mn^{3+} are canted in opposite direction. In this report, we have investigated $Pr_{1-x}Nd_xMnO_3$ compounds and it is interesting to observe how the magnetic properties change with doping of Nd ions in place of Pr.

2. Experimental

Polycrystalline samples of the composition, $Pr_{1-x}Nd_xMnO_3$ (x = 0·3, 0·5 and 0·7) were prepared in air via solid state reaction method. The precursors Pr_6O_{11}, Nd_2O_3 and MnO_2 were mixed in proper stoichiometric ratio. They were heated at 900 °C for 24 h. Then, the powder was pelletized and fired in air at 1500 °C for 24 h and the furnace was cooled down to room temperature at a rate of 100 °C/h. The room temperature crystal structure was determined by powder X-ray diffraction (XRD) measurements using CuKα radiation (Philips diffractometer). The lattice parameters were obtained from the Rietveld analysis of XRD data using FULLPROF program (Rodrigues-Carvajal *et al* 1993). Quantum design magnetometer was used to collect the a.c. magnetic susceptibility and d.c. magnetization data.

*Author for correspondence (sudipta.pal@rediffmail.com)

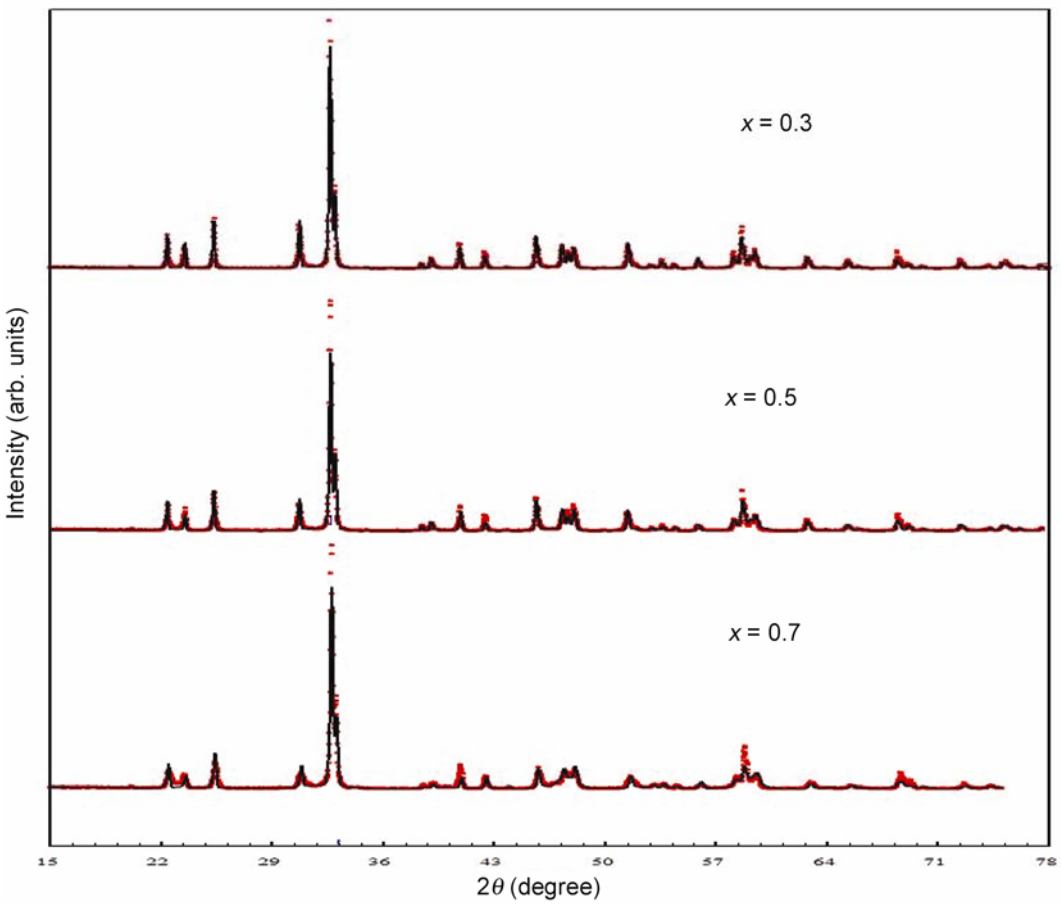

Figure 1. X-ray diffraction spectrum of $Pr_{1-x}Nd_xMnO_3$ (x = 0·3, 0·5 and 0·7).

Table 1. Values of lattice parameters of $Pr_{1-x}Nd_xMnO_3$.

Compounds	$a \pm 10^{-3}$ (Å)	$b \pm 10^{-3}$ (Å)	$c \pm 10^{-3}$ (Å)	$V \pm 10^{-3}$ (Å^3)
$Pr_{0.7}Nd_{0.3}MnO_3$	5·4378	5·8163	7·5749	239·5828
$Pr_{0.5}Nd_{0.5}MnO_3$	5·4316	5·8195	7·5687	239·2544
$Pr_{0.3}Nd_{0.7}MnO_3$	5·4239	5·7977	7·5597	237·7302

3. Results and discussion

Powder X-ray diffraction pattern, taken at room temperature and shown in figure 1, revealed a single phase orthorhombic *Pbnm* structure for all the samples. The lattice parameters are tabulated in table 1. For all concentrations, we obtained $b > a > c/\sqrt{2}$ indicative of a static JT distortion. The values of lattice parameters of present $Pr_{1-x}Nd_xMnO_3$ (x = 0·3, 0·5 and 0·7) solid solution are observed in between the values of end members $PrMnO_3$ and $NdMnO_3$ (Hemberger *et al* 2004). Very small change in the lattice parameters is observed with change of x. The lattice parameters decrease with the increase of x, which results from the substitution of smaller Nd^{3+} (1·08 Å) in place of Pr^{3+} (1·09 Å).

The temperature dependence of the a.c. susceptibility has been shown in figures 2(a and b). The in-phase and quadrature components of a.c. susceptibility (χ' and χ'') show a number of features. A well-defined peak is observed for all the compounds. There is well-defined maximum around 48 K in the x = 0·7 sample (i.e. $Pr_{0.3}Nd_{0.7}MnO_3$), which is assumed as a paramagnetic to ferrimagnetic transition according to earlier reports (Snyder *et al* 1997; Pena *et al* 2002). The width of the maximum broadened as well as shifted to the higher temperature with decrease of x and an additional maximum around 20 K is observed for x = 0·3 compound. It is remarkable to note that the anomalies associated with the magnetic ordering starts building at temperature around 85–95 K in the compounds. It is also observable that with decrease of Nd, both the values of χ' and χ'' decrease. In χ'' value, sharp peak is observed around 11–14 K depending on the composition of the compounds. Similar peak in χ'' has been reported in $NdMnO_3$ compound and it was

ascribed as the orientation of Mn spins (Wu *et al* 2000). The two anomalies, both in the real and imaginary susceptbility data for $x = 0{\cdot}3$ sample indicate that Mn orders at first antiferromagnetically with canted spin configuration and the rare earth moments subsequently couple antiferromagnetically with the canted moments of Mn.

It is interesting to note that due to the magnetic anisotropy in the sample at low temperature, the values of χ slightly deviated from Curie–Weiss behaviour. Above the transition temperature (T_{max}), χ shows a ferromagnetic character (as shown in figure 3) and follows a Curie–Weiss behaviour as for ferromagnetic system, $\chi = \mu_{eff}^2/[8(T-\Theta]$, with Θ positive. The value of Θ has been obtained as 54, 58 and 71 for $x = 0{\cdot}3$, $0{\cdot}5$ and $0{\cdot}7$, respectively. Positive paramagnetic temperature, Θ, is obtained for all the compounds by extrapolating $(\chi)^{-1}$ to 0 indicating the presence of ferromagnetic interaction in all the compounds. Now, from quantum mechanical spins μ_{eff} per mole for $Pr_{1-x}Nd_xMnO_3$ ($x = 0{\cdot}3$, $0{\cdot}5$ and $0{\cdot}7$) are 5·839, 5·958 and 6·074 μ_B, respectively. The Curie–Weiss law gives μ_{eff} per mole for $Pr_{1-x}Nd_xMnO_3$ ($x = 0{\cdot}3$, $0{\cdot}5$ and $0{\cdot}7$) which are 5·548, 5·429 and 5·774 μ_B, respectively. So, the experimental value agrees well with the theoretical estimation. Small deviation from the theoretical value could be explained considering that some of the ions |Pr + Nd| in the ferromagnetic network are aligned or canted in the direction of Mn ions due to the magnetic anisotropy in the compounds for doping.

Figure 4 provides temperature dependence d.c. magnetization of $Pr_{1-x}Nd_xMnO_3$ ($x = 0{\cdot}3$, $0{\cdot}5$ and $0{\cdot}7$). The d.c. magnetization has been measured in the external

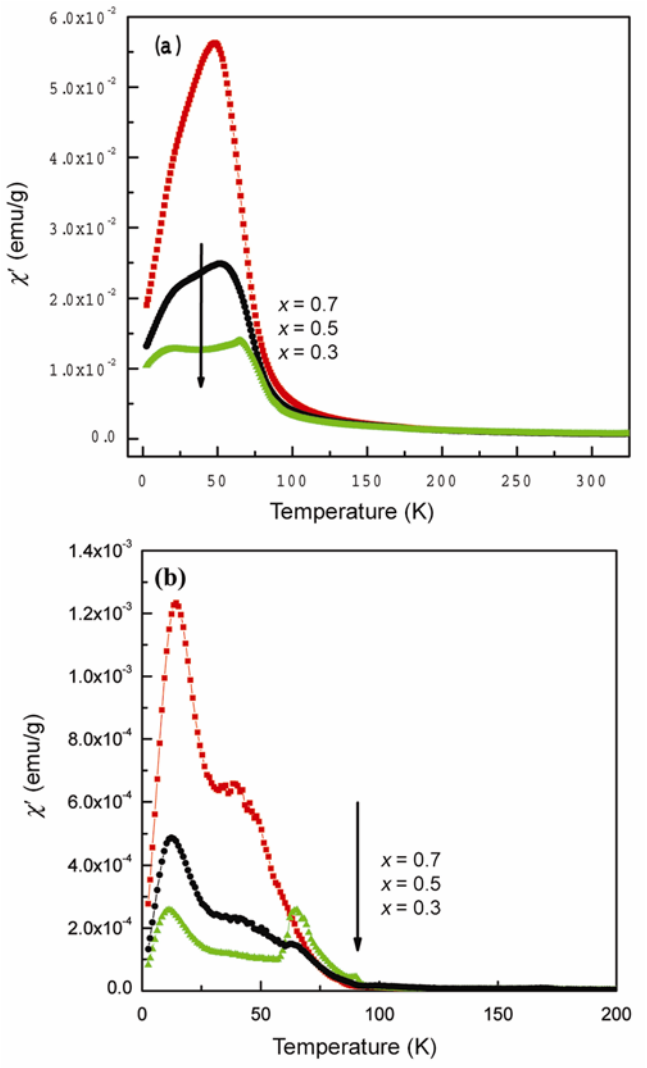

Figure 2. (**a**) Plot of *T*-dependent real a.c. susceptibility (χ') of $Pr_{1-x}Nd_xMnO_3$ ($x = 0{\cdot}3$, $0{\cdot}5$ and $0{\cdot}7$) compounds recorded at 10 Oe a.c. field and (**b**) plot of *T*-dependent imaginary a.c. susceptibility (χ'') of $Pr_{1-x}Nd_xMnO_3$ ($x = 0{\cdot}3$, $0{\cdot}5$ and $0{\cdot}7$) compounds.

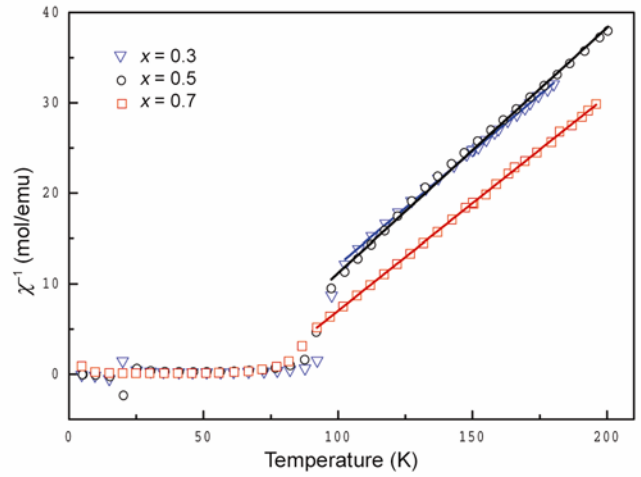

Figure 3. Temperature-dependent inverse d.c. susceptibility of $Pr_{1-x}Nd_xMnO_3$ ($x = 0{\cdot}3$, $0{\cdot}5$ and $0{\cdot}7$). Solid line is the high temperature fit using $\chi = \mu_{eff}^2/[8(T-\Theta)]$.

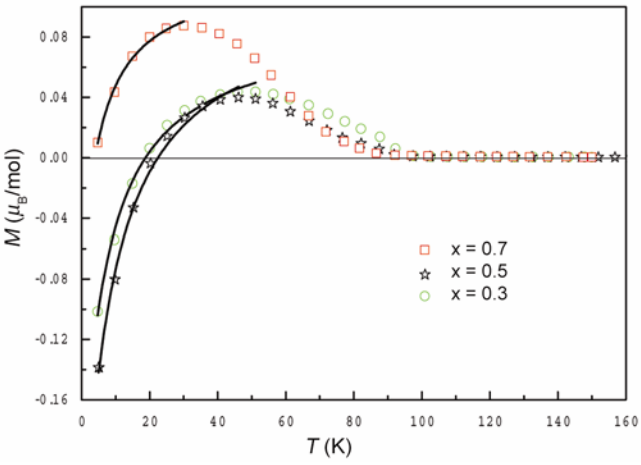

Figure 4. D.C. magnetization *M* vs temperature in $Pr_{1-x}Nd_xMnO_3$ ($x = 0{\cdot}3$, $0{\cdot}5$ and $0{\cdot}7$) in FC mode. Solid line shows Curie–Weiss type fitting of *M*–*T* data recorded in FC mode under 50 Oe.

Table 2. Fitting parameters for *M–T* curves recorded in FC mode.

Compounds	$M_{Mn} \pm 10^{-3}$ (μ_B/mol)	$H_{int} \pm 10^{-2}$ (Oe)	$\theta_w \pm 10^{-2}$ (K)
$Pr_{0·7}Nd_{0·3}MnO_3$	0·0897	–51·47	–7·33
$Pr_{0·5}Nd_{0·5}MnO_3$	0·1080	–52·08	–8·47
$Pr_{0·3}Nd_{0·7}MnO_3$	0·1237	–50·74	–5·65

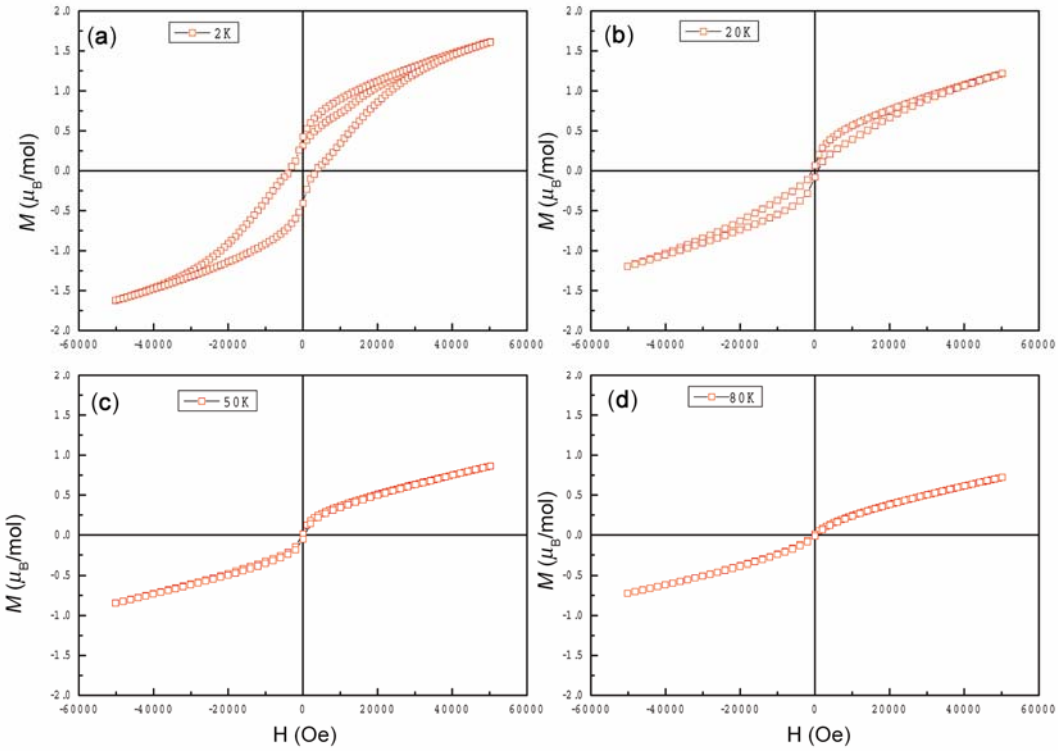

Figure 5. *M–H* curves recorded for $Pr_{0·5}Nd_{0·5}MnO_3$: (**a**) at 2 K, (**b**) at 20 K, (**c**) at 50 K and (**d**) at 80 K.

applied field 50 Oe in ZFC and FC processes. Interesting features can be observed in FC magnetization properties. In the sample, x = 0·3 and 0·5, FC magnetization becomes zero around 18 and 22 K, respectively. This can be considered as compensation point. FC magnetization goes through a positive maximum, before reaching the compensation point. The temperature at the maximum is considered as T_{max}. Upon further decrease of temperature, the magnetization becomes negative. At 5 K, the value of magnetization reaches –0·1 and –0·14 μ_B/mol for x = 0·3 and 0·5, respectively. FC magnetization in x = 0·7 sample does not show negative value up to 5 K.

The negative FC magnetization observed only in the solid solutions may have a correlation with the weakening of anisotropy around Pr^{3+}, arising from the substitution of Nd^{3+}. With decreasing temperatures, the Pr and Nd spins are more and more aligned in the opposite direction of the exchange field of the manganese moments, following a Curie-type temperature dependence and finally, yielding a negative magnetization at the lowest temperatures, when the polarization of the |Pr + Nd| spins exceeds FM component of Mn moments. The solid lines in figure 4(b) shows that the negative magnetization, M, can well be approximated by (Manna *et al* 2010; Sharma *et al* 2010):

$$M = M_{Mn} + \frac{C_{Nd}(H_{int} + H_{ext})}{T - \theta_W}, \quad (1)$$

where M_{Mn} is the canted moment of Mn, H_{int} the internal field due to the canted Mn moment, H_{ext} the applied field, C_{Nd} the Curie constant (1·59) and θ_w the Weiss constant. The limitation of this analysis is the assumption that M_{Mn} and H_{int} are independent of temperature, which is usually true, if $T << T_N$. In the present case, this may not be true and hence the value obtained will only be an approximation. The parameters obtained from the fitting using (1) are given in table 2. Similar results have been observed for $GdCrO_3$ (Yoshii 2001), $Bi_{0·3}Ca_{0·7}Mn_{0·75}Cr_{0·25}O_3$ (Zhang *et al* 2012), Sr_2YbRuO_6 (Singh and Tomy 2008) and $La_{0·5}Gd_{0·5}CrO_3$ (Sharma *et al* 2010). In these samples, negative magnetization is explained considering two

sublattices in opposite direction. The positive value of M_{Mn} is consistent with the result that FC magnetization goes through a positive maximum before reaching the compensation point and M_{Mn} was used as a fitting parameter and considered to be constant well below the temperature T_{max}. Actually, in our samples, the reversal of magnetization can easily be understood considering M_{Mn} is parallel to the applied field, while $M_{|Pr+Nd|}$ are antiparallel to it. As the temperature decreases, the disordered |Pr + Nd| ions begin to polarize against the canted field of M_{Mn} moments. As a result, the net magnetization of the system is $M_S = M_{Mn} - M_{|Pr+Nd|}$. As the temperature decreases from T_{max}, $M_{|Pr+Nd|}$ increases much faster than M_{Mn}. At the compensation point of magnetization, the two sublattices are equal and net magnetization becomes zero. And below the compensation temperature, the net magnetization becomes negative.

For better understanding of the magnetic property, field-dependent magnetization measurement has been performed at some particular temperature, signifying each magnetic phase identified from the *M–T* curve on one of the samples with $x = 0{\cdot}5$. The measurements were performed after cooling the sample in zero field and the results have been shown in figure 5. It is observed that at 80 K, the *M–H* curve does not show hysteresis, however, it shows a nonlinear nature, indicating a ferrimagnetic behaviour. *M–H* curve at 50 K, where the maximum in FC magnetization occurs, is similar to the earlier one, with small increase in magnetization value. A small hysteresis is observed at 20 K with coercive field (H_C) of 800 Oe. The hysteresis increases with lowering of temperature and at 2 K, a better hysteresis curve formed with coercive field (H_C) of 3600 Oe. The hysteresis loops in figure 5 clearly shows that these loops are symmetric about the origin. This indicates absence of the exchange bias field for the sample in zero field cooled condition. Similar magnetization behaviours have been observed earlier in Nd based manganites (Hong *et al* 2012). It is noticeable that magnetization does not reach to saturation value in the *M–H* curve. This may be due to the spin canting of ions in the magnetic sublattice along with large magnetic anisotropy in the sample.

4. Conclusions

The low-temperature magnetization reversal in the compound $Pr_{1-x}Nd_xMnO_3$ has been investigated. The interaction between two interacting networks of Pr/Nd and Mn ion largely changes, this may be due to the spin canting of ions in the magnetic sublattice along with large magnetic anisotropy in the sample. The relative effect of each sublattice's magnetization due to local internal field at the Mn site and negatively aligned Mn spins with respect to the |Pr + Nd| ferromagnetic moments varies with temperature and leads to a spin reversal when the magnetic moment of the ferromagnetic network sublattice is larger than the Mn moment.

Acknowledgements

The authors acknowledge experimental assistance from Laboratoire CRISMAT, UMR 6508, CNRS/ ENSICAEN, Caen Cedex, France and DST FAST TRACK project no. SR/FTP/PS-101/2010, Govt. of India.

References

Biswas S, Khan M H, Pal S and Bose E 2013 *J. Magn. Magn. Mater.* **328** 31

Hemberger J, Lobina S, von Nidda H A K, Ivanov V Y, Mukhin A A, Balbashov A M and Loidl A 2004 *Phys. Rev.* **B70** 024414

Hong F, Cheng Z, Wang J, Wang X and Dou S 2012 *Appl. Phys. Lett.* **101** 102411

Hemberger J *et al* 2004 *Phys. Rev.* **B69** 064418

Mandal P, Serrao C R, Suard E, Caignaert V, Raveau B, Sundaresan A and Rao C N R 2013 *J. Solid State Chem.* **197** 408

Manna P K *et al* 2010 *J. Phys: Conf. Series* **200** 072063

Pena O, Bahout M, Ghanimi K, Duran P, Gutierrez D and Moure C 2002 *J. Mater. Chem.* **12** 2480

Rodrigues-Carvajal J 1993 *Physica* **B192** 55

Sharma N, Srivastava B K, Krishnamurthy A and Nigam A K 2010 *Solid State Sci.* **12** 1464

Singh R P and Tomy C V 2008 *J. Phys.: Condensed Matter* **20** 235209

Snyder G J, Booth C H, Bridges F, Hiskes R, Dicarolis S, Beasley M R and Geballe T H 1997 *Phys. Rev.* **B55** 10

Wu *et al* 2000 *J. Appl. Phys.* **87** 9

Yoshii K 2001 *J. Solid State Chem.* **159** 204

Yoshii K, Nakamura A, Ishii Y and Morri Y 2001 *J. Solid State Chem.* **162** 84

Zhang R R *et al* 2012 *J. Alloys Compd.* **519** 92

Zhang S, Tan S, Tong W and Zhang Y 2005 *Phys. Rev.* **B72** 014453